SUPPLEMENTARY INFORMATION

1 The *FGS* Data Set

There are three *FGS* on board of *HST* . Each *FGS* consists of four photomultipliers (PMTs). Nominal *HST* operation uses two *FGS* for guiding, with each *FGS* observing its own guide star. The photon counts recorded by each *FGS* are therefore different, but global instrumental artifacts and Observatory level transients will display in both *FGS* and can therefore be identified and removed.

Observations of the inclination distribution of large KBOs find that about 75% have an inclination angle $|i| \lesssim 20^\circ$ [29, 30, 31]. We therefore divide the *FGS* observations into a low ecliptic latitude ($|b| < 20^\circ$) and a high ecliptic latitude ($|b| > 20^\circ$) sample. The high-ecliptic latitude observations ($|b| > 20^\circ$) provide an excellent control sample.

2 *FGS* Guide Stars

The *FGS* guide stars span a broad range of magnitudes and spectral types. The signal-to-noise ratio, S/N, in a 1/40 s data bin depends on the magnitude of the star. Its distribution is shown in Supplementary Figure 1.

The angular sizes of guide stars were derived by fitting the 2MASS [32] JHK and USNO-B1 BR [33] photometry with a black-body spectrum. Supplementary Figure 2 shows the angular radii distribution of the guide stars. About 66% of the stars in our data set subtend angular sizes less than 0.5 of the Fresnel scale at a distance of 40 AU. The diffraction pattern that is produced by a sub-km sized KBO occulting an extended background star is smoothed over the finite stellar disk. This effect becomes clearly noticeable for stars that subtend sizes larger than about 0.5 of a Fresnel scales [34, 35] and it reduces the detectability of occultation events around such stars. The effect of finite angular radii of the guide stars on the detection efficiency of our survey is taken into account (see Detection Efficency section 5 for details).

3 Detection Algorithm

Our detection algorithm performs a template search with theoretical light curves and uses a χ^2 fitting procedure to identify occultation candidates. Our survey is most likely to detect KBO occultation events caused by objects that are 200-500 m in radius given the signal-to-noise of our data and for a power-law index of the KBO size distribution, q, between 3 and 4.5. Occultation events in this size range are in the Fraunhofer regime. The theoretical light curves for our search algorithm are therefore calculated in the Fraunhofer regime. Our templates are calculated for various impact parameters assuming a point source background star and are integrated over the 400-700 nm wavelength range of the *FGS* observations. For a given impact parameter between the KBO and the star, our theoretical light curves have three free parameters that we fit for. The first is the mean number of photon counts, which is the normalization of the light curve. The second is the amplitude of the occultation, which is proportional to the size of the KBO, and the third is the width of the occultation, which is independent of the object size, and is determined by the ratio of the Fresnel scale to the relative speed between *HST* and the KBO perpendicular to the line of sight. This relative speed is determined by the combination of *HST* 's velocity around the Earth, Earth's velocity around the Sun and the velocity of the KBO itself. We use this information to restrict the parameter space for the template widths in our search such that we are sensitive to KBOs located at the distance of the Kuiper belt between 30 AU and 60 AU.

4 Detection Criterion and Significance Estimates

The significance of occultation candidates can be measured by their $\Delta\chi^2$ which is defined here as the difference between the χ^2 calculated for the best fit of a flat light curve, which corresponds to no event, and the χ^2 of the best fit template. Occultation events have large $\Delta\chi^2$, since they are poorly fit by a constant. Cosmic ray events, which give rise to one very large photon count reading in a 40 Hz interval, can also result in a large $\Delta\chi^2$ but the fit of the occultation template is very poor. We examined all flagged events for which the template fit of the diffraction pattern was better than $15\,\sigma$. About a

handful of false-positives where flagged by our detection algorithm that have a value of $\Delta\chi^2$ comparable to or larger than the occultation event. However, in *all* cases these false-positives were caused by a 1 Hz jitter due to the displacement of the guide star from its null position. The occultation event itself did not show any such jitter. To determine the $\Delta\chi^2$ detection criterion for our search algorithm and to estimate the probability that detected events are due to random noise we use the bootstrap technique [36]. Specifically, from a given *FGS* time series of length N we randomly selected N points with repetitions and created 'artificial' time series from it. We analyzed these 'artificial' data sets using the same search algorithm that we applied to the actual *FGS* data. This technique creates random time series with noise properties identical to those of the actual data, but it will lose any correlated noise. Therefore, this technique is justified if there is no correlated noise in the data sets. To look for correlated noise we calculated the auto-correlation function, with lags between 0 to 1 s. Most of the data sets are free of statistical significant correlated noise. The $\sim 12\%$ of the data sets that did show correlated noise exceeding $4\,\sigma$, which was often due to slopes (e.g., long-term variability) in the data sets, were excluded from the bootstrap analysis.

The *FGS* data set consists of observations of many different stars with magnitudes ranging from 9 to 14. The number of photon counts and signal-to-noise properties vary therefore from observation to observation (see Supplementary Figure 1 for the signal-to-noise ratio distribution of the FGS observations). Our $\Delta\chi^2$ calculation accounts for the Poisson noise of the data. Therefore, the probability that occultation candidates are due to random noise can be characterized by a single value of $\Delta\chi^2$ for all observations, irrespective of the mean photon count of a given observation provided that the noise properties across all observations are well characterized by a Poisson distribution. In reality, the noise properties are different from observation to observation; especially non-Poisson tails in the photon counts distribution will give rise to slightly different $\Delta\chi^2$ distributions. Therefore, ideally, we would determine a unique detection criterion for each individual data set. However, this would require to simulate each data set, which contains about an hour of observations in a single *HST* orbit, over the entire length of our survey ($\sim 12,000$ star hours). This is not feasible due to the enormous computational resources that would be required, i.e. simulating a single one hour data set over the entire survey length requires about 5 CPU days, which

corresponds to $\sim 60,000$ CPU days for the entire *FGS* survey. Instead, we perform the bootstrap simulation over all the *FGS* data sets together, where each individual data set was simulated about a 100 times, which required about ~ 500 CPU days in total. This way we estimate the typical $\Delta\chi^2$ value that corresponds to having less than one false-positive detection over the $\sim 12,000$ star hours of low ecliptic observations. For all occultation candidates that exceed this detection threshold, we determined their statistical significance, i.e. the probability that they are due to random noise, by extensive bootstrap simulations of the individual data sets (Supplementary Figure 5).

5 Detection Efficency

The ability to detect an occultation event of a given size KBO depends on the impact parameter of the KBO, the duration of the event, the angular size of the star and the signal-to-noise ratio of the data. We determined the detection efficiency of our survey by recovering synthetic events that we planted into the observed photometric time series by multiplying the actual *FGS* data with theoretical light curves of KBO occultation events. The synthetic events correspond to KBO sizes ranging from $130\,\mathrm{m} < \mathrm{r} < 650\,\mathrm{m}$, they have impact parameters from 0 to 5.5 Fresnel scales and a relative velocity distribution that is identical to that of the actual *FGS* observations. To account for the finite angular sizes of the stars we generated light curve templates with stellar angular radii of 0.1, 0.2, 0.3, 0.4, 0.6, 0.8 and 1 Fresnel scales distributed as shown in Supplementary Figure 2. The modified light curves with the synthetic events were analyzed using the same search algorithm that we used to analyze the *FGS* data. The detection efficency of our survey was calculated using the angular size distribution of the *FGS* guide stars assuming a distance of 40 AU. We normalize our detection efficency for a given size KBO, $\eta(r)$, to 1 for an effective detection cross section with a radius of one Fresnel scale.

The detection efficiency of our survey is ~ 0.05 (~ 0.6) for objects with $r = 200\,\mathrm{m}$ ($r = 500\,\mathrm{m}$) located at 40 AU. Note that this value for the detection efficency already accounts for the angular radii distribution of the guide stars (e.g., for comparison, stars that subtend angular radii less than 0.5 of the Fresnel scale result in a detection efficency of ~ 0.08 [~ 0.8] for objects with $r = 200\,\mathrm{m}$ [$r = 500\,\mathrm{m}$].).

6 Calculating the KBO Surface Density

The number of occultation events is given by

$$N_{events} \simeq -2 v_{rel} F \int_{r_{min}}^{r_{max}} \int_{-b}^{b} \eta(r) \frac{\Delta t}{\Delta b} \frac{dN(r,b)}{dr} \, \mathrm{dbdr} \tag{1}$$

where $v_{rel} = 23\,\mathrm{km/s}$ is the typical relative velocity between the KBO and the observer, b is the ecliptic latitude, $\Delta t/\Delta b$ is the time observed per degree in ecliptic latitude (see Supplementary Figure 3) and $F = 1.3\,\mathrm{km}$ is the Fresnel scale. The number density of KBOs is both a function of ecliptic latitude and the KBO radius, r. Here we assume that the KBO latitude distribution, $f(b)$, is independent of size and we take the distribution provided in Elliot et al. (2005) [31]. We further assume that the KBO size distribution follows a power law. It can therefore be written as $N(r,b) = n_0 \times r^{-q+1} \times f(b)$ where n_0 is the normalization factor for the cumulative surface density of KBOs. Substituting for $dN(r,b)/dr$ in equation 1 and solving for n_0 we have

$$n_0 \simeq \frac{N_{events}}{2 v_{rel} F (q-1) \int_{r_{min}}^{r_{max}} \eta(r) r^{-q} \, \mathrm{dr} \int_{-\mathrm{b}}^{\mathrm{b}} \mathrm{f(b)} \frac{\Delta \mathrm{t}}{\Delta \mathrm{b}} \, \mathrm{db}}. \tag{2}$$

Evaluating equation 2 yields a cumulative KBO surface density averaged over the ecliptic ($|b| < 5^\circ$) of

$$N(r > 250\,m) \simeq 2.1 \times 10^7 \,\mathrm{deg}^{-2} \tag{3}$$

We assumed $q = 4$ when evaluating the integral over r. We note however that the value for the cumulative KBO surface density at $r = 250\,\mathrm{m}$ only depends weakly on the exact choice for q [e.g. $N(r > 250\,m)$ only ranges from $2.3 \times 10^7\,\mathrm{deg}^{-2}$ to $2.1 \times 10^7\,\mathrm{deg}^{-2}$ for values of q between 3 and 4.5]. We quote our results as the KBO surface density of objects larger than 250 m in radius since this is roughly the size of KBOs, which our survey is most likely to detect given our detection efficency and a power-law size distribution with $q = 3 - 4.5$. The implied surface density for KBOs with radii larger than 250 m is $7.7 \times 10^6\,\mathrm{deg}^{-2}$ at $b = 5.5^\circ$, which is the ecliptic latitude of the RXTE observations of Scorpius X-1, and it is $4.4 \times 10^6\,\mathrm{deg}^{-2}$ for $8^\circ < |b| < 20^\circ$.

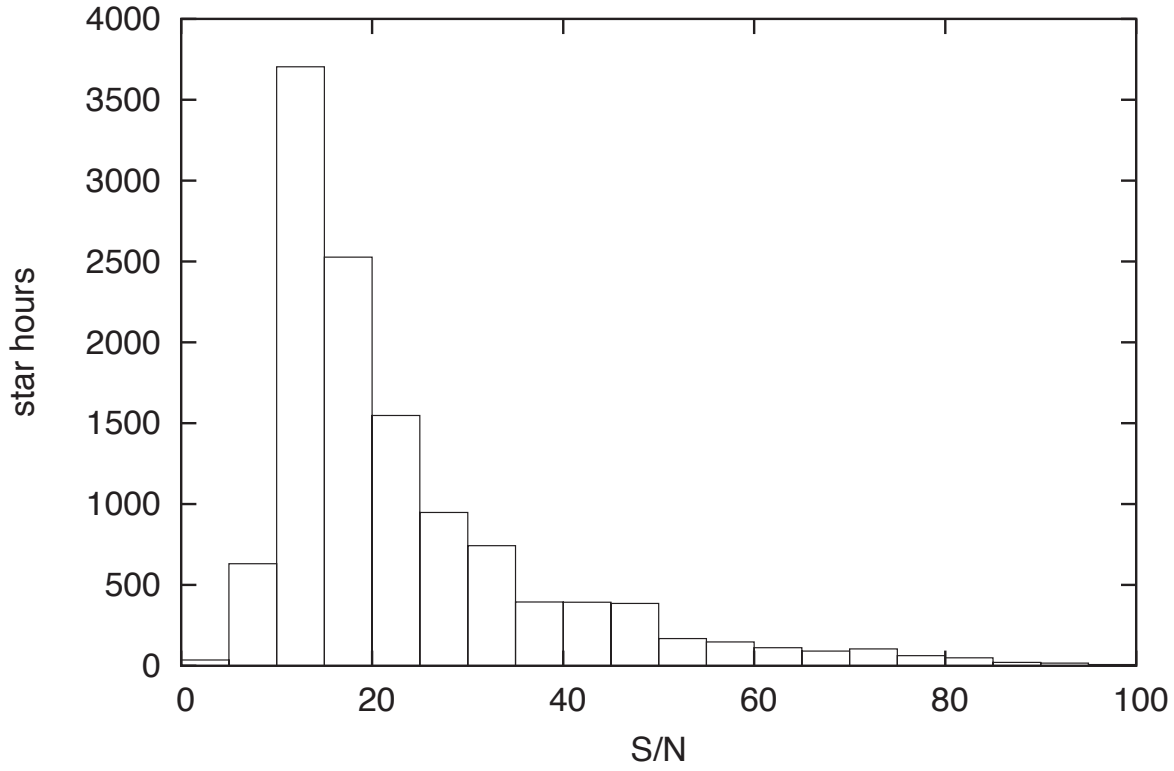

Supplementary Figure 1: Distribution of star hours as a function of the mean signal-to-noise ratio, S/N, in a 40 Hz bin for the 12,000 hours of low ecliptic latitude observations ($|b| < 20°$) in the analyzed FGS data set.

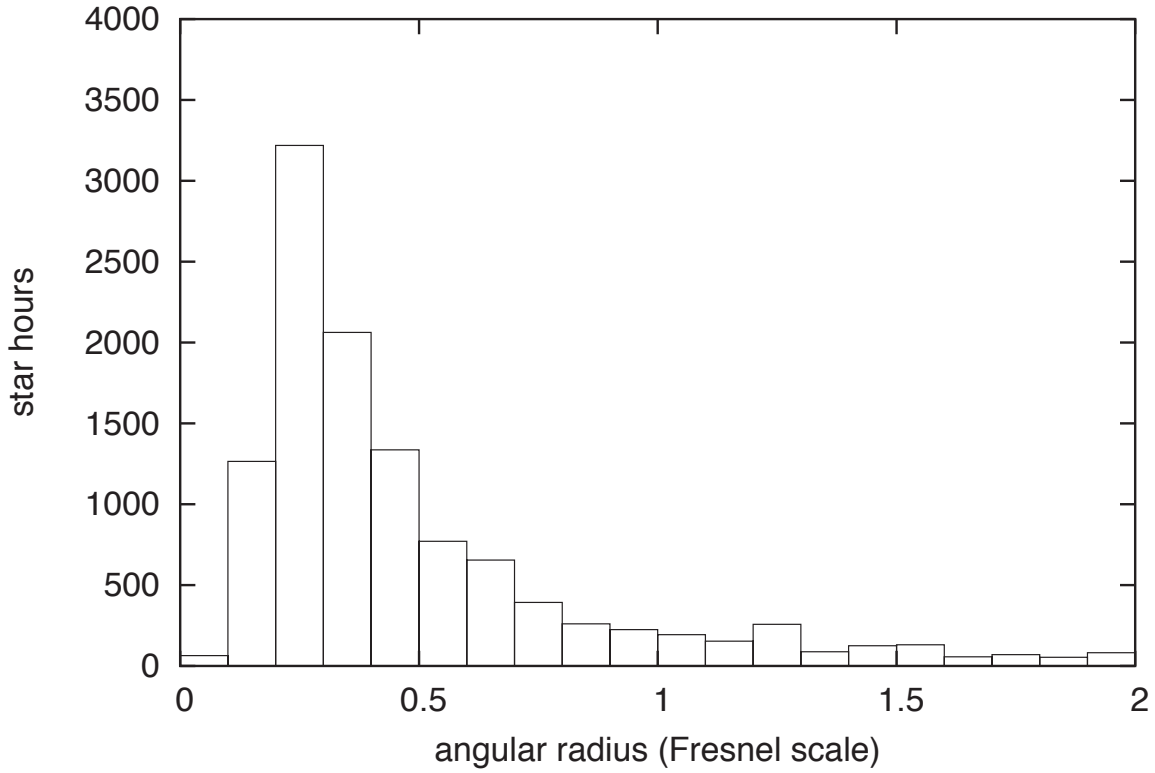

Supplementary Figure 2: Distribution of star hours as a function of angular radii of the guide stars. The angular radii are given as fraction of the Fresnel scale both which are calculated at 40 AU.

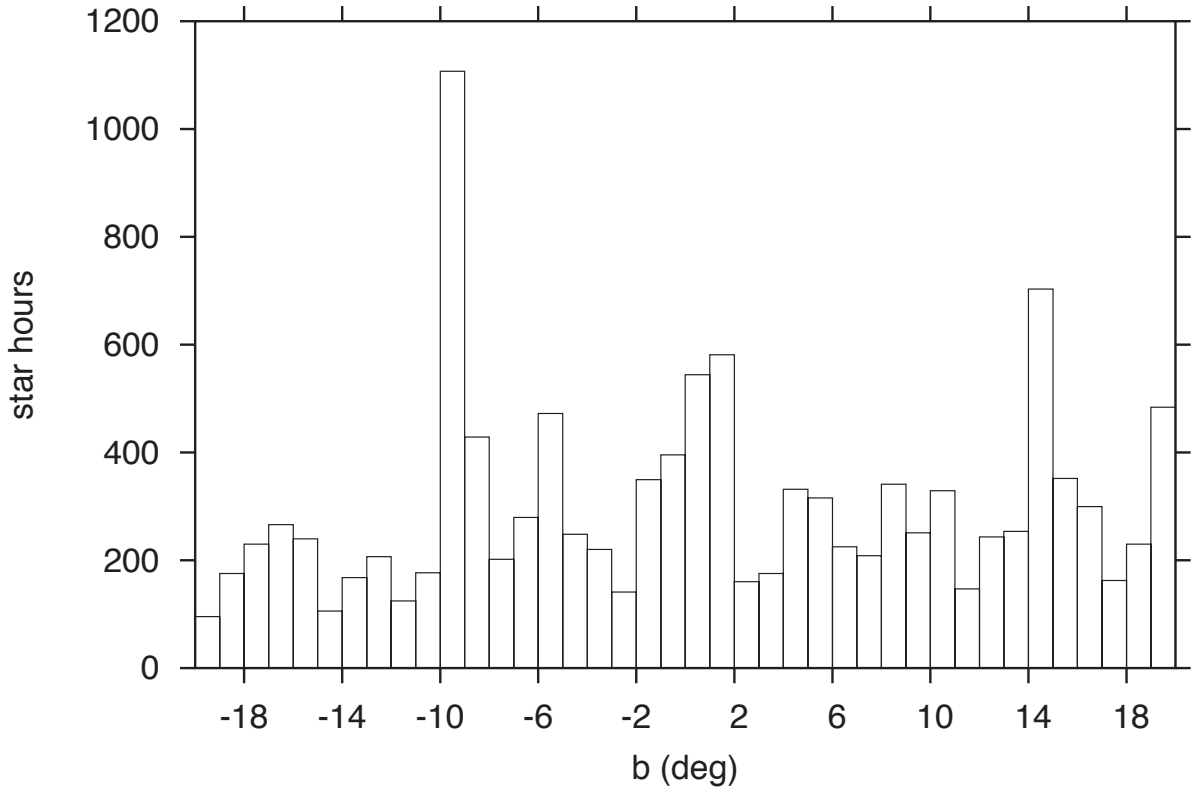

Supplementary Figure 3: Distribution of star hours as a function of ecliptic latitude, b, for the 12,000 hours of low ecliptic latitude observations ($|b| < 20°$) in the analyzed FGS data set.

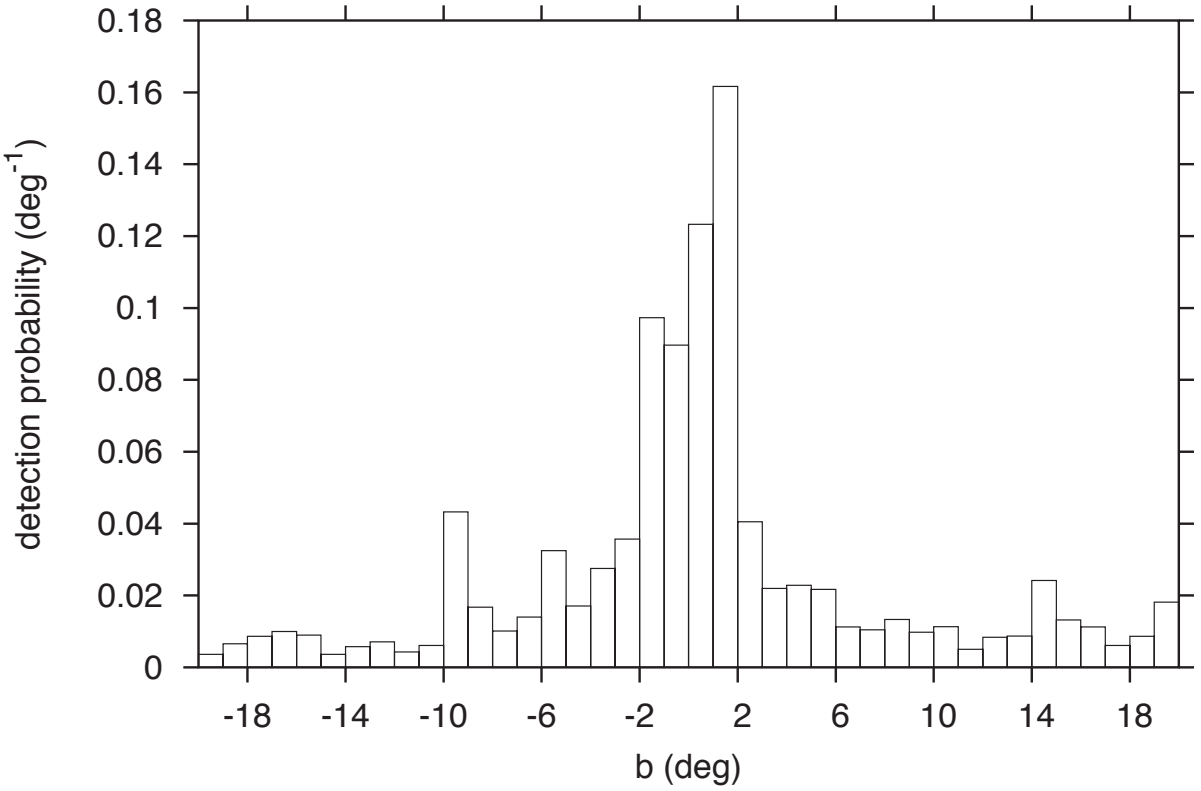

Supplementary Figure 4: Detection probability as a function of ecliptic latitude, b, for the 12,000 hours of low ecliptic latitude observations ($|b| < 20°$) of the analyzed FGS data set. The detection probability was calculated from the ecliptic latitude distribution of FGS guide stars shown in Supplementary Figure 3 and the KBO ecliptic latitude distribution from Elliot et al. (2005)[31]. Note, we assumed that the KBO ecliptic latitude distribution is symmetric about the ecliptic and ignored the small $\sim 1.6°$ inclination of the Kuiper belt plane[31] relative to the ecliptic. For our survey, there is $\sim 60\%$ probability that KBO occultations will occur inside the low-inclination core region ($|b| < 4°$) of the Kuiper belt. The probability for KBO occultations outside the core region is roughly uniform for $4° < |b| < 20°$ and about 40% of all KBO occultations will occur outside the low-inclination core region. The detection of one object at 14° is therefore consistent with the latitude distribution of our observations and that of KBOs.

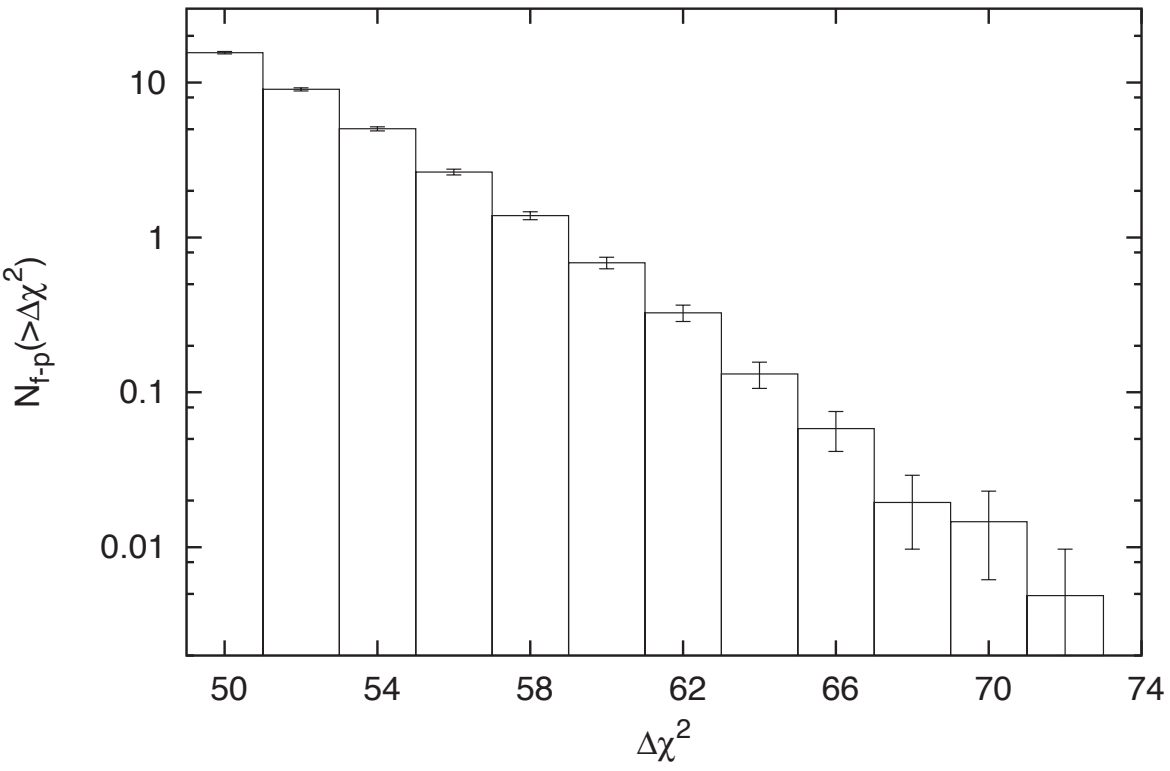

Supplementary Figure 5: Cumulative number of false-positives, N_{f-p}, as a function of $\Delta\chi^2$. These false-positives were obtained from bootstrap simulations using data from $\sim$ 28 minutes of *FGS* observations that were acquired over one *HST* orbit, in which we discovered the occultation candidate. The original time series was 32 minutes long and we removed the last 4 minutes that showed a significant increasing trend in the number of photon counts. We removed the occultation event itself (which occurred about 2.3 minutes before the start of the trend) and simulated 2.5×10^6 star hours, which is 206 times larger than our low ecliptic latitude observations. This calculation required $\sim$ 1400 CPU days of computing power. The number of false-positives, N_{f-p}, was normalized to 12,000 star hours, which corresponds to the length of the entire low ecliptic latitude observations. In the entire bootstrap analysis we obtained 4 events with a $\Delta\chi^2 \geq 67.3$. This implies a probability of 8×10^{-7} that events like the occultation candidate with $\Delta\chi^2 = 67.3$ are caused by random statistical fluctuations within the original 32 minutes data set that contained the event and a probability of $\sim 4/206 \sim 2\%$ that events like the occultation candidate are caused by random statistical fluctuations over the entire low ecliptic latitude observations. The analysis of our high ecliptic latitude control sample, which is twice as large, did not yield any events that were comparable in significance to the occultation candidate.

References

[29] Jewitt, D., Luu, J. & Chen, J. The Mauna Kea-Cerro-Tololo (MKCT) Kuiper Belt and Centaur Survey. *Astron. J.* **112**, 1225–1238 September 1996.

[30] Brown, M. E. The Inclination Distribution of the Kuiper Belt. *Astron. J.* **121**, 2804–2814 May 2001.

[31] Elliot, J. L., Kern, S. D., Clancy, K. B., Gulbis, A. A. S., Millis, R. L. *et al.* The Deep Ecliptic Survey: A Search for Kuiper Belt Objects and Centaurs. II. Dynamical Classification, the Kuiper Belt Plane, and the Core Population. *Astron. J.* **129**, 1117–1162 February 2005.

[32] Skrutskie, M. F., Cutri, R. M., Stiening, R., Weinberg, M. D., Schneider, S. *et al.* The Two Micron All Sky Survey (2MASS). *Astron. J.* **131**, 1163–1183 February 2006.

[33] Monet, D. G., Levine, S. E., Canzian, B., Ables, H. D., Bird, A. R. *et al.* The USNO-B Catalog. *Astron. J.* **125**, 984–993 February 2003.

[34] Roques, F. & Moncuquet, M. A Detection Method for Small Kuiper Belt Objects: The Search for Stellar Occultations. *Icarus* **147**, 530–544 October 2000.

[35] Nihei, T. C., Lehner, M. J., Bianco, F. B., King, S.-K., Giammarco, J. M. *et al.* Detectability of Occultations of Stars by Objects in the Kuiper Belt and Oort Cloud. *Astron. J.* **134**, 1596–1612 October 2007.

[36] Efron, B. *The Jackknife, the Bootstrap and other resampling plans.* Society for Industrial Mathematics (1982).